PHYSICAL REVIEW B **67**, 165211 (2003)

Analysis of the sharp donor-acceptor pair luminescence in 4*H*-SiC doped with nitrogen and aluminum

I. G. Ivanov, B. Magnusson,* and E. Janzén

Department of Physics and Measurement Technology, Linköping University, S-581 83 Linköping, Sweden

(Received 9 December 2002; published 30 April 2003)

We analyze the sharp lines in the donor-acceptor (nitrogen-aluminum) emission spectrum in 4H-SiC by means of a fit with theoretically calculated spectra. The theory accounts for the anisotropy and the presence of inequivalent sites in this polytype of SiC, and it is shown that the predominant emission in the linear part of the spectrum is due to pairs involving nitrogen donor and aluminum acceptor at hexagonal sites. The fit allows determination of the ionization energy of the aluminum at hexagonal site, 199 ± 2 meV, which is in excellent agreement with the results obtained using free-to-bound spectra.

DOI: 10.1103/PhysRevB.67.165211 PACS number(s): 71.55.−i, 71.35.−y, 78.55.Hx

I. INTRODUCTION

It is well known that the analysis of the multiple-line spectrum arising from recombination of carriers bound to a neutral donor-acceptor pair (DAP) can yield important parameters of both the host material (the dielectric constant),[1,2] as well as the ionization energies of the donor and acceptor species involved. The analysis is based on the formula[3]

$$\hbar\omega_{PL}=E_g-(E_D+E_A)+\frac{e^2}{\varepsilon R}+J(R), \tag{1}$$

where $\hbar\omega_{PL}$ is the energy of the photon emitted during the recombination and registered as photoluminescence (PL), E_g, E_D, and E_A are the electronic band gap, and the donor and acceptor binding energies of the ground state (ionization energies), respectively, e is the electron charge, ε is the dielectric constant of the host material, R is the distance between the donor and acceptor, and $J(R)$ denotes all the corrections to the initial state of the pair (neutral donor and acceptor) and its final state (ionized donor and acceptor). $J(R)$ is usually unknown, but it vanishes for large R much faster than the Coulomb term. This makes possible the fitting of the spectrum for intermediate values of R by Eq. (1) with $J(R)$ set to zero. Such a fit provides rather accurate value of the quantity $\hbar\omega_\infty=E_g-(E_D+E_A)$ (the photon energy corresponding to $R\to\infty$), as well as identification of the discrete values of $R(m)$ corresponding to different shell numbers m.[3] After the shell identification is obtained, the fit can be improved by including multipole correction terms in $J(R)$,[1,4,5] which account for the deviation of the charges of the ionized donor and acceptor from a point charge. Their net effect is splitting of a line associated with certain shell number into several lines, corresponding to arrangements of the donor and acceptor along inequivalent crystal directions. The value of the splitting vanishes rapidly with increasing R because the leading term is proportional to R^{-4}.[4] This procedure has been employed successfully on various cubic semiconductors where sharp emission lines due to DAP-PL can be resolved (GaP,[1,3] 3C-SiC,[5,6] etc.). To the best of our knowledge, the fit has been successful only on cubic crystals with isotropic ε. Attempts to analyze the sharp lines due to DAP luminescence in the uniaxial crystal CdS (wurtzite structure) have been restricted to correlation of the density of lines in the experimental and calculated spectra.[7,8] In Ref. 7 it was shown that due to anisotropy this hexagonal crystal (CdS) has a much more complicated structure of the DAP spectrum than a cubic crystal. In addition to the anisotropy, 4*H*-SiC (and higher hexagonal polytypes) also possesses inequivalent lattice sites, which makes the structure of the DAP spectrum even more complicated (see Sec. III A). Probably for this reason the analysis of the DAP-PL in uniaxial polytypes of SiC [4*H*, 6*H*,[9,10] and 15*R* (Ref. 10)] is usually restricted to the discussion of broadband DAP luminescence.

The 4*H* polytype of SiC was chosen as a subject of this study because it is a simple uniaxial polytype with only two inequivalent lattice sites (per substitutional donor or acceptor), and because samples of high quality with widely varying doping levels are readily available. Besides, despite the wide industrial interest in this material, its fundamental properties are far from being well established (e.g., the dielectric constant, or the exact knowledge of donor and acceptor binding energies). From this point of view, investigation of the *sharp* emission arising from donor-acceptor (D-A) pairs is quite relevant.

This paper presents a more detailed analysis of the structure of the DAP luminescence spectrum in 4*H*-SiC made on the ground of a fit with theoretical spectra. The samples and the experimental details are described in Sec. II. An account on the features arising from the anisotropy and the presence of inequivalent lattice sites in 4*H*-SiC is done in Sec. III. The results from the fitting of the DAP spectrum originating from N-donor–Al-acceptor pair recombination are discussed in Sec. IV. (These donor and acceptor species are chosen as most common ones.) A revision of their ionization energies is carried out on the ground of the fit of the DAP spectrum and the free-to-bound spectra. An estimate of the value of the dielectric permittivity in 4*H*-SiC is made as well. The conclusions are summarized in Sec. V.

II. SAMPLES AND EXPERIMENTAL DETAILS

Four 4*H*-SiC samples were chosen for this study. The parameters of the samples are presented in Table I. All of them were bulk *p*-type material intentionally doped with Al. The nitrogen doping is the background level, and it is at least two orders of magnitude lower in the material grown by high temperature chemical vapor deposition (samples No. 1 and

 ©2003 The American Physical Society

TABLE I. Parameters of the samples. All doping levels are in units cm^{-3}.

Sample number	Al concentration	N concentration	Net-acceptor concentration [a]
1 [b]	4.8×10^{17} [c]	$\leqslant10^{15}$ [d]	2.2×10^{17}
2 [b]	4.0×10^{18} [c]	$\leqslant10^{15}$ [d]	2.8×10^{18}
3 [e]	$>9\times10^{17}$ [d]	$\geqslant10^{17}$ [d]	9×10^{17}
4 [e]	$>2\times10^{18}$ [d]	$>10^{17}$ [d]	2×10^{18}

[a]From capacitance-voltage measurement at 300 K.
[b]Grown by high-temperature chemical vapor deposition.
[c]Measured using secondary ion mass spectroscopy.
[d]Estimated according to supplier specifications.
[e]Al-doped *p*-type bulk material from CREE Inc., USA.

No. 2). Therefore, although the Al doping level is of the same order of magnitude in samples No. 2 and No. 3, but the donor-acceptor pair concentration is much higher in the latter sample due to the higher content of nitrogen.

The photoluminescence spectra were taken at temperature $T\approx2$ K using 351.14-nm UV excitation from an Ar-ion laser. The detection was either with a Jobin-Yvon monochromator (HR460) coupled with a charge-coupled device camera, with resolution (full width at half maximum, FWHM) of 0.5 Å, or with a double monochromator (SPEX 1404) and photomultiplier, with resolution 0.3 Å or less. However, using a better resolution did not show sharper DAP lines, probably because some doping-induced strain is always present in the samples, and it leads to weak homogeneous broadening of each line, which is of the same order as the linewidth of the spectrometer transfer function (0.3–0.5 Å).

All samples showed the same structure of the linear part of the spectrum arising from recombination of relatively close pairs. Although the total magnitude of the DAP spectrum increases with the doping (for a fixed excitation power), the weight of the linear part of the spectrum decreases at the same time, as will be seen in Sec. III B. The sharp DAP lines are most prominent in sample No. 1, which has lowest-doping level. Thus, the spectra of this sample No. 1 were used for fitting.

III. THEORETICAL ASPECTS

A. Specific features of 4*H*-SiC

The following features have to be considered in the case of 4*H*-SiC.

(1) The crystal is uniaxial so the dielectric constant is a tensor with two different components: $\varepsilon_\parallel$ (along the crystal *c* axis) and $\varepsilon_\perp$ (perpendicular to it). The Coulomb term $E_C=e^2/\varepsilon R$ in Eq. (1) has to be modified to

$$E_C=\frac{e^2}{\sqrt{\varepsilon_\parallel\varepsilon_\perp}\sqrt{x^2+y^2+\frac{\varepsilon_\perp}{\varepsilon_\parallel}z^2}}\cong\frac{e^2}{\varepsilon R}\left(1+\frac{\varepsilon_\parallel-\varepsilon_\perp}{2\varepsilon_\parallel}\frac{z^2}{R^2}\right), \quad (2)$$

where $\mathbf{R}=(x,y,z)$ is the radius vector from the donor to the acceptor (*z* axis is oriented along the crystal *c* axis), $R=|\mathbf{R}|$, and $\varepsilon=\sqrt{\varepsilon_\parallel\varepsilon_\perp}$. The accuracy of the right-hand approximation in Eq. (2) is better than 0.1%, provided the value $\triangle\varepsilon=(\varepsilon_\parallel-\varepsilon_\perp)/\varepsilon_\parallel$ does not exceed 0.04. This is the case for 6H-SiC, where $\triangle\varepsilon=0.037$ ($\varepsilon_\parallel=10.03$ and $\varepsilon_\perp=9.66$),[21] and we anticipate that the (unknown) values for 4*H*-SiC are not very different from those of 6*H*. Equation (2) shows that even without considering the multipole corrections mentioned above, each line in the spectrum corresponding to a shell with given *R* will split into lines corresponding to subshells with different values of *z*. Moreover, the maximum value of the splitting [equal to $(e^2/\varepsilon R)(\varepsilon_\parallel-\varepsilon_\perp)/2\varepsilon_\parallel$] does not decay rapidly with increasing *R*, and therefore cannot be neglected for any value of *R*, in contrast to the correction terms included in $J(R)$.

(2) There exist two inequivalent sites for either the donor (N on carbon site, N_C) or the acceptor (Al on Si site, Al_{Si}), usually denoted as *h* (hexagonal) and *k* (cubic). Since the ionization energy of the donor or acceptor is site dependent, doping with a single dopant (e.g., N donor) introduces two donor energy levels. We denote the donor (*D*) or acceptor (*A*) on a hexagonal (cubic) site as D_h or A_h (D_k or A_k, respectively). The corresponding ionization energies are denoted as E_{Dh}, E_{Ah}, E_{Dk}, and E_{Ak}, respectively. Therefore, one donor (N) and acceptor (Al) species gives rise to four different sets of DAP-PL lines, corresponding to four types of isolated pairs: D_h-A_h, D_h-A_k, D_k-A_h, and D_k-A_k, all with different values for the term (E_D+E_A) in Eq. (1). We denote by *hh* set the set of lines corresponding to donor and acceptor on hexagonal sites (D_h-A_h), and similarly we define the *hk* and *kk* sets. Obviously, the shells for the sets *hk* (D_h-A_k) and *kh* (D_k-A_h) coincide as a sequence of the lattice geometry. However, the corresponding sets of lines in the PL spectrum do not coincide being shifted from each other for large values of *R* [so that $J(R)\approx0$] by the energy value $(E_{Dk}+E_{Ah})-(E_{Dh}+E_{Ak})$, in accord to Eq. (1).

In addition, we note that the number of shells below a certain value of *R* is larger in 4*H*-SiC than in the cubic 3*C*-SiC (see also Ref. 7, where the authors compare the shells of the wurtzite structure with these in a hypothetic cubic structure). For example, $R\approx21.66$ Å corresponds to shell number 50 in 3*C*-SiC, but to shell numbers 89 and 98 in the *hk* and *hh* sets, respectively (provided the "ideal" c/a ratio is considered, where *c* and *a* are the lattice constants in the direction of the *c* axis and in the basal plane).

The above circumstances increase the multitude of observed lines if compared to a cubic crystal. Especially, complications in identification of individual lines arise from the fact that the spectrum consists of four interpenetrating sets of lines (*hh*, *hk*, *kh*, and *kk*). Nevertheless, we will show in the next paragraph that there are reasons to expect significantly different amplitudes in the contribution of the different sets to the spectrum. This provides a ground for identification of at least this set, which dominates the spectrum.

B. Capture cross-section dependence on the donor-acceptor separation

A model qualitatively describing the two-step process of capture of an electron and a hole by ionized *D*-*A* pairs is

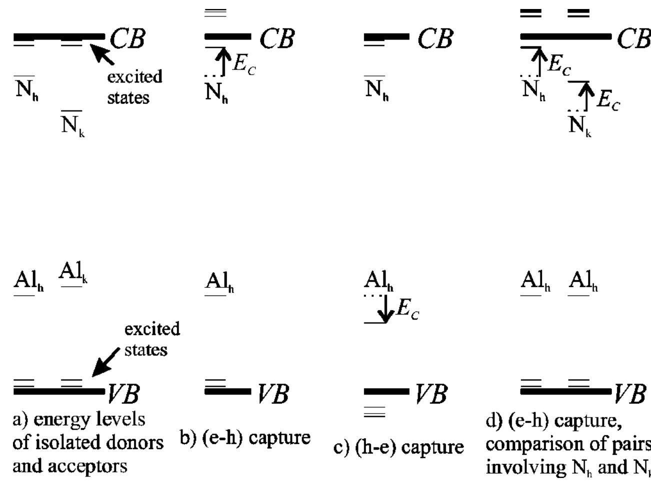

FIG. 1. Energy diagram of the donor and acceptor levels discussed in the text: (a) energy levels of the isolated N donors and Al acceptors in 4H-SiC, at hexagonal (N_h,Al_h) and cubic (N_k,Al_k) sites; (b) energy levels of N_h in the presence of ionized acceptor Al_h at a distance R when the electron is captured first; (c) energy levels of Al_h in the presence of ionized donor N_h at a distance R when the hole is captured first; (c) comparison of an N_h-Al_h pair and an N_k-Al_h pair separated by the same distance R for the case of electron first capture. VB and CB denote the top of the valence band and the bottom of the conduction band, respectively.

described in Ref. 11. This model has consequences in the case of one donor species with two different ionization energies corresponding to the two inequivalent lattice sites, so we give below a brief account on it and adapt it to the case of 4H-SiC.

In the following, we use the notations introduced by Dean and Patrick[11] to discuss the capture modes in the two-step capture process of an electron and a hole by a donor-acceptor pair. Thus, $\sigma_1(e-h)$ denotes the capture cross section for the first step (therefore, subscript one) when the electron is captured first [therefore $(e-h)$]. The cross sections $\sigma_1(h-e)$, $\sigma_2(e-h)$, and $\sigma_2(h-e)$ are defined in a similar manner.[11] Dean and Patrick show that, in general, σ_1 exhibits abrupt changes in its dependence on the donor-acceptor pair separation R, whereas σ_2 does not. From the point of view of their model, we consider the specific case of 4H-SiC.

The energy levels to which an electron (a hole) can be captured by an isolated donor (acceptor) are schematically sketched in Fig. 1(a) for both the hexagonal and cubic sites. Let us regard, for instance, the donor and acceptor at hexagonal sites. If they are involved in a D-A pair separated by a certain distance R, then their levels can be pictured in two different ways, shown in Figs. 1(b) and (c), depending on whether the electron is captured first [Fig. 1(b)] or the hole [Fig. 1(c)]. If the first step is capture of an electron, then to the first approximation [meaning neglecting of $J(R)$] the energy levels of the donor can be pictured as the energy levels of an isolated donor but shifted towards the conduction band by the value of the energy of the Coulomb interaction between the donor and acceptor, $E_C = e^2/\varepsilon R$ [see Fig. 1(b)]. The case in Fig. 1(b) corresponds to such R that all shifted donor states are degenerate with the conduction band, except for the ground state, which is then the only state capable of binding an electron. (In classical terms, the repelling force from the negatively charged acceptor does not allow binding of the electron in states with too large orbits.) When the electron is bound to the donor ground state and the donor becomes neutral, the acceptor levels can be considered as undisturbed [bottom of Fig. 1(b)] if we neglect the polarization interaction of the acceptor with the neutral donor. Thus, the second capture step, i.e., the capture of the hole by the ionized acceptor, can occur into any of its excited (or ground) states. According to Lax mechanism of capture,[12] it is the capture to excited states which is responsible for the large capture cross section of ionized impurities, so the capture cross section for the second step, $\sigma_2(e-h)$, will be large. Consequently, the second capture is much faster than the first so that the total time for capture of both carriers by the pair is governed by the first capture (of electron, in this case). The situation is reversed in Fig. 1(c), where the case of first capture of a hole is considered. Similarly, the second capture is fast [$\sigma_2(h-e)$ is large].

It is natural to ask the question which of the two capturing sequences (e-h or h-e) depicted above occurs faster and, therefore, is more probable? It is known that the Al-acceptor ionization energies in SiC ($\sim$200 meV, or more)[10,13] are significantly larger than those for the N donor at any site.[10,14] Consequently, the donors in SiC have larger Bohr radii than the acceptors. One can expect that the cross section for capture to the ground state will scale roughly as the square of the Bohr radius r_0 of this state if the excited states are within the band. Since for the hydrogen atom $r_0 \propto 1/E_0$, where E_0 is the energy of the ground state, one can take as a rough estimate $r_{0D}^2/r_{0A}^2 \sim E_A^2/E_D^2 \gg 1$, where r_{0D} (r_{0A}) is the Bohr radius of an unspecified donor (acceptor). This makes plausible the conclusion that $\sigma_1(e-h)/\sigma_1(h-e) \gg 1$. We underline that this inequality holds only if capture to excited states is not possible, which means that the Coulomb term is greater than the binding energy of the first excited state E_{i2} for both the donor and the acceptor.[11]

Let us compare now the capture cross sections for N_h and N_k in the case when $E_C > E_{i2}$. From Fig. 1(d), it is easy to see that there exists a rather wide region of separations R, for which only capture to the ground state of either donor is available. The ionization energy of the shallower donor N_h ($E_{Dh} \approx 61.4$ meV)[15] is about half of that of N_k.[10,14] Hence, the ground state of N_h has a larger Bohr radius, and larger capture cross section for electrons. One can expect that capturing to pairs involving N_h is more probable than to pairs involving N_k. In addition, the recombination at such pairs (N_h-Al_h or N_h-Al_k) is faster, also due to the larger Bohr radius of the ground state. It is natural to conclude that recombination at such pairs will dominate the DAP spectrum.

If the pair separation is so small that the Coulomb energy E_C is larger than the ionization energy of either donor, still two mechanisms for capture of carriers are available. The first is the less probable mechanism of capturing first the hole (to the acceptor ground state), and afterwards the electron. The second possibility is direct capture of an exciton by the pair.[16]

Let us consider now the limit of very distant pairs when the Coulomb term is less than the energies of many excited states, which means enabled capture to these states. The corresponding capture cross section is estimated to vary as $1/R^2$ in this case,[11] i.e., the capture cross section for remote pairs is much larger than for close pairs [both $\sigma_1(e-h)$ and $\sigma_1(h-e)$ are larger]. Furthermore, as long as the excited states are involved, we do not expect a strong site dependence of the capture cross section as in the case of close pairs. However, we do expect the the recombination rate of distant pairs involving N_k is very different from the recombination rate of distant pairs involving N_h because the recombination rate depends exponentially on the Bohr radius of the donor *ground* state:

$$1/\tau_{k,h} \propto \exp(-R/R_{k,h}), \tag{3}$$

where τ_h (τ_k) is the average lifetime before recombination of the pair at a distance R, involving donor at hexagonal (cubic) site, respectively, and R_h, R_k are half the corresponding Bohr radii for the ground state of the donor.[17] Consequently, for a certain excitation level, remote pairs involving the shallower donor N_h will be populated much less than those involving the deeper one (N_k), simply because their depopulation rate is much faster.

This consideration finds its experimental confirmation in the power dependence of the DAP spectrum (apart from the well-known shift of the broad DAP luminescence peak with the excitation power), and in the dependence of the DAP luminescence on the doping level. It is well known that the lines associated with close pairs only appear when the crystals have reasonably low donor and acceptor concentrations and when they are intensively excited.[18] However, the explanation in Ref. 18 only addresses the much greater optical transition probability of the close pairs, and not their much smaller capture cross section, if compared to the remote pairs. Here we complete this explanation. Regarding the power dependence, at very low-excitation levels, mainly the broad peaks due to very remote pairs are observed. This is seen by comparing the spectra *a* and *c* of sample No. 1 in Fig. 2, taken with low- and high-excitation power (cf. also curves *b* and *e*, referring to sample No. 3). In the low-excitation case [Fig. 2 (curves *a* and *b*)], the remote pairs outcompete the closer ones in capturing the few light-excited carriers, and the luminescence from close pairs, which gives rise to sharp lines in the spectrum, disappears (or becomes negligible). The remote pairs need to be saturated in order to enable the observation of photoluminescence from close pairs. Their saturation at higher power excitation is favored both by their low recombination rate (due to exponentially small probability for charge transfer from the donor to the acceptor) and large capture cross section. Under saturation condition, the large capture cross section of the remote pairs is disabled because they spend most of the time in their neutral state. Thus, there will be many light-generated excess free carriers available for capture by close pairs.

The large difference in the capture cross section of close and remote pairs is involved also in the explanation of the doping dependence of the DAP spectrum. At certain fixed excitation level, the saturation of remote pairs will be stronger for low-doped crystals than for high-doped crystals, simply because their concentration is lower at low doping. This is illustrated in Fig. 2 (curves c–f), where the spectra of four samples with different doping levels, taken with the same rather high-excitation level ($\sim$50 W/cm^2, focused laser beam at 351.1 nm), are compared. Although the concentration of close pairs also increases with doping, we observe *decrease* of the weight of the sharp lines associated with their recombination in the spectrum because the remote pairs become less saturated and easily outcompete the closer pairs in capture.

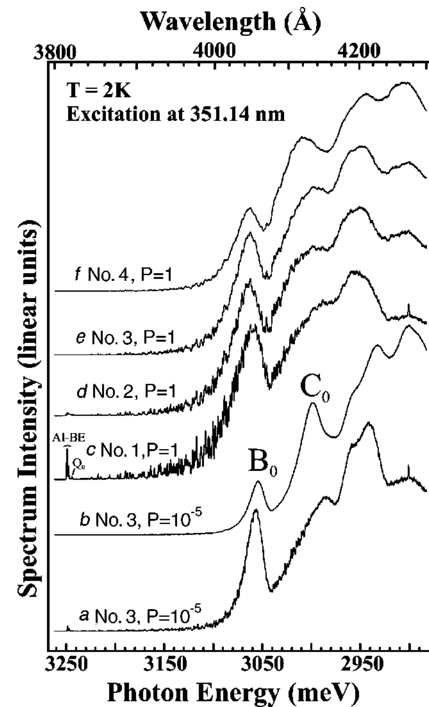

FIG. 2. PL spectra of the four $4H$ samples. Each spectrum is labeled with the sample number (No. 1, etc.) and the approximate excitation power P ($P=1$ corresponds to $\approx$50 W/cm^2). The sharp lines, which are most prominent in curve *c*, are due to recombination from close pairs. The broad peaks denoted B_0 and C_0 are due to remote-pair recombination involving N_h and N_k, respectively, and the remaining broadbands are phonon replicas of these peaks. The lines denoted Al-BE and Q_0 arise from recombination of excitons at neutral acceptors and donors, respectively. All spectra are normalized to their maxima.

When inequivalent lattice sites are present, as in the case of $4H$-SiC, more than one peak associated with remote pairs is observed. In Fig. 2 (curves *a* and *b*), the spectra of samples No. 1 and No. 3 are compared, recorded with the same very low-excitation power (about 5 mW/cm^2), in order to promote the observation of the remote-pair peaks. The peak denoted B_0 is known to be due to recombination at remote pairs involving the shallower donor N_h, whereas the C_0 peak is due to recombination at remote pairs involving N_k.[9,10] Since sample No. 3 is higher doped than No. 1, we anticipate lower saturation in that sample. Indeed, the C_0 peak is hardly visible in sample No. 1, which means a high saturation level for this peak even at this low excitation, but it dominates the spectrum of sample No. 3. (Note that the

close-pair related sharp lines also appear for sample No. 1, albeit weakly, which again indicates high saturation.) However, the B_0 peak is prominent in both samples, which clearly illustrates the difference in the saturation level for pairs involving N_h and N_k. Since the capture cross section for remote pairs involving N_h or N_k is about the same,[19] the difference in their saturation is attributed mainly to the larger optical transition probability of pairs involving the shallower donor N_h. It is worth noting that raising the excitation power saturates the C_0 peak also in sample No. 3, as can be seen by comparing the spectra of this sample in Fig. 2 (curves b and e). In addition, at high power excitation, the relative amplitude of C_0 is largest in the most highly doped sample No. 4, see Fig. 2 (curve f), in agreement with the lowest saturation level of the remote-pair peaks in this sample.

IV. RESULTS FROM THE FIT AND DISCUSSION

A. Fit of the sharp DAP emission

Our intention is to fit a part of the DAP spectrum corresponding to intermediate values of R, when line structure still exists, but the correction term $J(R)$ can already be considered as negligible. Due to the features of 4H-SiC depicted in Sec. III A, it is necessary to model the spectrum for *hk*, *hh*, and *kk* sets and then fit each of them separately to the experimental spectrum. Even for a single set, the lines already merge at intermediate R due to the presence of many more shells than in a cubic crystal (and subshells within many of the shells). Therefore, the modeling of the spectrum must include broadening of each line by, for instance, the linewidth of the spectrometer transfer function. Only the Coulomb term is included in the model in the form presented by Eq. (2). The peaks obtained in such way are added together and the model spectrum is obtained. A similar approach with simulated spectra has been used to fit the DAP-PL of very remote pairs (up to $R\sim70$ Å) in GaP,[2] and ZnSe.[20]

The values for 6H-SiC $\varepsilon=9.84$ and $\triangle\varepsilon=0.037$ were chosen initially,[21] and varied afterwards. Each of the sets (*hh*, *hk*, and *kk*) has been simulated separately and the simulated spectrum has been moved along the experimental one in order to find a correlation between the simulated and observed peaks by means of a special computer program.

Only a part from each set has been used for the fit, corresponding approximately to $40<E_C<60$ meV (or ~25 Å $<R<37.5$ Å, shell numbers from ≈100 up to 330). An estimate of the multipole corrections can be made for $R\sim25$ Å if we use the constants obtained for 3C-SiC.[5] It turns out that the maximum values of the multipole corrections V_3 and V_4 (see Ref. 5) for this distance do not exceed 0.5 and 0.2 meV, respectively. We assume that these estimations are also applicable to 4H-SiC, thus justifying the neglecting of $J(R)$.

Another approximation to be mentioned is the use of the "ideal" ratio, $(c/a)_{ideal}=4\sqrt{2}/\sqrt{3}$. The real ratio is somewhat larger (by 0.17%), however, when we use it to calculate the sets, their shape does not exhibit any visual change (except for the closest pairs, which are not used in the fit anyway). We prefer then to use the ideal ratio, since this greatly

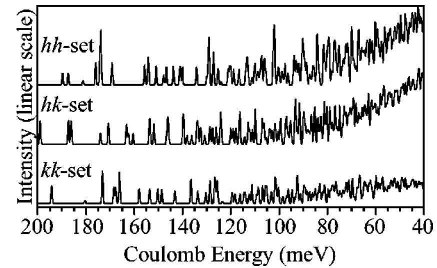

FIG. 3. Synthesized spectra for the three sets of DAP lines. The spectral intensity is proportional to the number of atoms in a subshell, which have the same value for E_C, and corrected with an exponential factor, as explained in text.

reduces the number of shells to be considered and simplifies the calculations. The value for the lattice constant in the basal plane $a=3.073$ Å at room temperature was corrected to zero temperature using its dependence on temperature. The latter is available in the literature only for 6H-SiC,[22] but is assumed to be valid also for 4H-SiC, thus $a=3.0723$ Å was used as the value at 2 K. However, this correction also did not produce any visual change in the shape of the simulated spectra.

The simulated spectra are shown in Fig. 3. In synthesizing the spectra, the broadening of each line is taken to be 0.55 meV (FWHM), in order to achieve best visual agreement with the experimental spectra. This value is slightly larger than the linewidth of the spectrometer transfer function (≈0.4 meV), which accounts for some stress-related broadening of the lines due to doping even in the spectra of sample No. 1 with the lowest-doping level. The broadening increases with the doping, as can be seen from Fig. 2. Furthermore, each simulated spectrum is multiplied by an exponential factor of the form $\exp(-E_i/E_C)$, where $E_i=2e^2/\varepsilon R_{Di}$ is some characteristic energy, different for the *hh* and *hk* sets, on one side, and the *kh* and *kk* sets on the other side, because the donor radii R_{Di} are different (the index i is either h, or k for the donor at hexagonal and cubic sites). This factor accounts for the exponentially decreasing recombination probability with increasing R (decreasing E_C), see Eq. (3).[17] Here we denote the set of lines associated with N_h-Al_k pairs as *hk* set to distinguish from the set of lines associated with the N_k-Al_h pairs denoted as *kh*. Apart from the exponential factor, these sets are the same so only the *hk* set is shown in Fig. 3. The value of $E_h=130$ meV ($R_{Dh}\approx17.2$ Å) was found to reproduce reasonably the intensities of the experimental lines in the *hh* set (see below). The value $E_k=200$ meV was used for the *kh* and *kk* sets.

Among the three sets (*hh*, *hk*, and *kk*), the *hh* set provides best fit to the spectrum in the region ≈3063–3088 meV, as shown in detail in Fig. 4. It turns out that the agreement between the peak positions in the experimental and simulated curve is relatively sensitive to the value of ε. The best agreement is obtained for values between 9.90 and 10.00. This allows estimation of the static dielectric constant $\varepsilon=9.95\pm0.10$ in 4H-SiC. The fit is not very sensitive to variations of $\triangle\varepsilon$ in the limits 0.036–0.044, thus we estimate $\triangle\varepsilon=0.04\pm0.005$. For comparison, the values for 6H-SiC are $\varepsilon=9.84$ and $\triangle\varepsilon=0.037$, according to literature.[21]

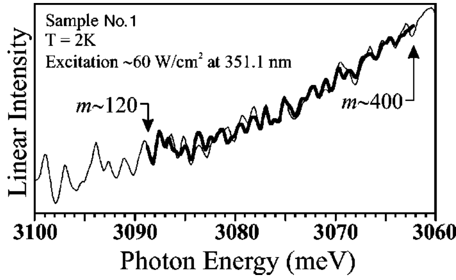

FIG. 4. Fit of the experimental spectrum (thin line) with the theoretical *hh* set alone (thick line). Approximate shell numbers *m* are shown at the limits of the fitted region.

All peaks in the theoretical curve have corresponding peaks in the experimental one. Note that the discrepancy between theory and experiment diminishes with decreasing E_C (increasing R), as should be expected in view of the decrease of $J(R)$. There are almost no unfitted peaks in the experimental curve, which leads to the conclusion that this part of the spectrum is indeed dominated by *D*-*A* recombination involving (N_h-Al_h) pairs, in agreement with the consideration in Sec. III B.

The region of variation of E_C used for the fit is chosen to be less than $E_{Dh}=61.4$ meV and larger than the binding energies of donor excited states, as discussed in Sec. III B. We can now examine how well the *hh* set fits to the experimental spectrum at higher energies, as shown in Fig. 5 (see the *hh* set). It is easy to see that even for $E_C>61.4$ meV and up to at least 85 meV, the theoretical curve (the *hh* set solely) describes well most of the features in the spectrum, and no sharp intensity cutoff is observed. Thus N_h-Al_h pair recombination is dominating the whole energy region 40 meV $<E_C<85$ meV. It is possible to find correlation with the *hh* set for even higher energies, but the increasing shifts due to the increase of $J(R)$ make the direct assignment difficult. These observations indicate that the cross section for capture of excitons is also largest for the N_h-Al_h pairs, if compared to the other possible pairs.

A value of $\hbar\omega_\infty(N_h-Al_h)=E_g-(E_{Dh}+E_{Ah})=3027$ meV is obtained by the fit. It is probably accurate within 1 or 2 meV because ε is not known exactly and $J(R)$ is neglected. Since $E_{Dh}=61.4$ meV is known,[15] and $E_g\approx3287$ meV,[23] we deduce the acceptor binding energy $E_{Ah}\approx(3287-3027-61.4)=198.6$ meV. This value is in excellent agreement with our measurements of free-to-bound spectra, shown in Sec. IV B, and in good agreement with the values of 191 meV (Ref. 10) and 203 meV,[13] obtained earlier. (These values will be discussed again in the following section in connection with the free-to-bound spectra.) From the fit we identify this acceptor as Al acceptor at *h* site and estimate its ionization energy $E_{Ah}\approx199\pm2$ meV at 2 K.

The fact that the spectral region shown in Fig. 4 contains predominantly emission from N_h-Al_h pairs is in conflict with the assumption of almost equal ionization energies of the two acceptors, Al_h and Al_k, suggested in Ref. 10. If this assumption was valid, the spectrum would show contributions from both *hh* and *hk* sets with nearly equal amplitudes as a consequence of the almost equal Bohr radii for the acceptors. Thus, the agreement solely with the *hh* set is a hint that Al_k has larger binding energy, smaller Bohr radius, and, consequently, smaller capture cross section and radiation rate, which would explain the negligible contribution of the *hk* set in the spectral region upon consideration. We discuss this possibility in some detail.

Where observable, the N_h-Al_k pair emission should fit the *hk* series, which applies also for the N_k-Al_h pairs (to distinguish them, we denoted the theoretical set of lines by *kh* set in the latter case). The value of $\hbar\omega_\infty(N_k-Al_h)$ for the latter can be estimated using $E_{Ah}\approx199$ meV, and estimating E_{Dk} from the difference $\triangle E\approx55$ meV between the maxima of the B_0 and C_0 peaks [see Fig. 2 (curve *b*)] associated with recombination from remote pairs involving the deeper C_0 and the shallower B_0 nitrogen donors:[10] $E_{Dk}\approx E_{Dh}+\triangle E\approx117$ meV. Indeed, the *kh* set provides a satisfactory fit around the energy region 3014–3034 meV, which can be seen in Fig. 5 (the *kh* set). The value $\hbar\omega_\infty(N_k-Al_h)\approx2974$ meV is obtained, hence $E_{Dk}\approx114$ meV, in reasonable agreement with the above estimate. Another correlation of the *hk* set with the experimental spectrum was found in the region 3040–3054 meV, also shown in Fig. 5 (see the *hk*

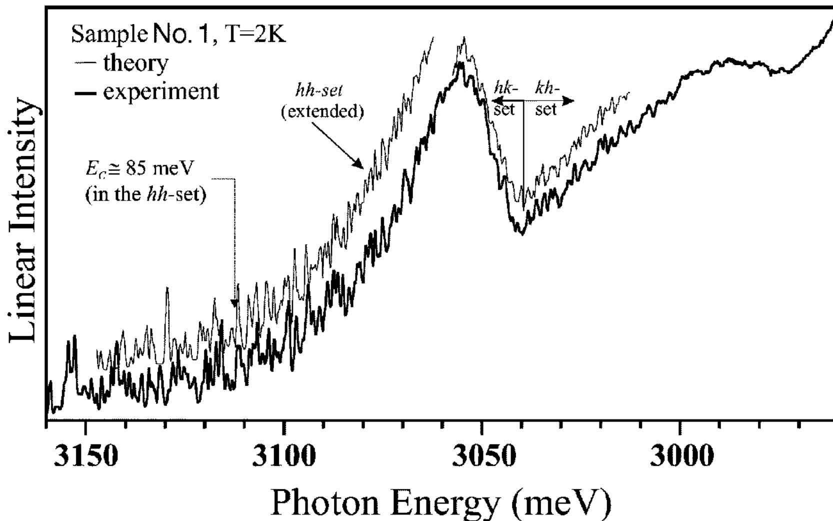

FIG. 5. General view of the fit of the experimental spectrum with the *hh*, *hk*, and *kh* sets. The higher-energy region of the *hh* set is shown in order to illustrate the good correlation with the experimental spectrum up to energies $E_C\sim85$ meV. The theoretical curves are shifted vertically to separate them from the experimental spectrum.

set), which yields the value of $\hbar\omega_\infty(N_h - Al_k) = E_g - (E_{Dh} + E_{Ak}) \approx 2998$ meV. This leads to $E_{Ak} \approx 228$ meV. Unfortunately, the quality of the latter two fits is worse than the fit with the *hh* set. That is why the fit with the *hk* set cannot be used to decide unambiguously the existence of the deeper Al_k level. This is due partly to the weakness of the lines, and partly to the underlaying background and overlap with other no-phonon sets or phonon replicas of the (N_h-Al_h) set, which fall in the same spectral region. For similar reasons, it is not possible to examine the fit with the *kk* set, which would occur at lowest energies [by estimate, $\hbar\omega_\infty(N_k - Al_k) \approx 2945$ meV] if the hypothesis of deeper Al_k level around 228 meV is valid.

Finally, the recombination of remote pairs involving Al_k should be a subject of stronger saturation than for pairs involving Al_h because the overlap of the wave functions of the electron on the donor and the hole on the acceptor will be smaller if Al_k is involved (assuming that it indeed has larger ionization energy and smaller Bohr radius). This might explain the absence of other remote-pair related broadbands than B_0 and C_0. Note that also in other polytypes of SiC, for example, 6*H*- and 15*R*-SiC, the number of broadbands does not correspond to the number of possible sets of donor-acceptor pairs, although it is shown that the Al acceptor has rather well pronounced site dependence of its ionization energy for these polytypes.[10]

B. Free-to-bound spectra

Free electrons from the conduction band, which are available at elevated temperatures due to partial thermal ionization of the donors, can make transition to recombine with the holes bound to the acceptors (free-to-bound transitions). The recombination is radiative with photon energy $\hbar\omega_{FB} = E(k) - E_A$, where $E(k)$ is the initial energy of the electron (with Boltzmann distribution near the bottom of the conduction band), and E_A is the acceptor ionization energy. Such free-to-bound spectra have already been observed in several polytypes of SiC, for both Al and B acceptors.[10,24–26] The free-to-bound spectrum provides a means of estimating the acceptor ionization energy.[10,13] However, we have to review the value of 203 meV deduced in Ref. 13. We have to reconsider also the assumption made in Ref. 10 regarding the equal ionization energies for Al_h and Al_k in 4*H*-SiC.

The free-to-bound spectra for two of our samples at temperatures between 70 and 100 K are shown in Fig. 6. The position of the maximum of the known free-to-bound peak (marked FB_1) is 3093 meV, close to the positions reported before.[10,13] If the line shape of the FB peak suggested in Ref. 10 is used, this maximum is positioned at $E_g - E_A + \frac{1}{2}kT$. Hence, $E_g - E_A \approx 3088.7$ meV because the Boltzmann factor $kT \approx 4.3$ meV at 100 K. Consequently, if $E_g = 3287$ meV, then $E_A \approx 198.3$ meV. We attempted also a fit of this peak, which yielded the value $E_G - E_A = 3088.5$ meV. These values for $E_G - E_A$ are slightly underestimated because we do not account for the slight decrease of the band gap with temperature. Therefore, they are in close agreement with the value 3089 meV, obtained in Ref. 13, where the band gap narrowing with temperature is taken into account. However,

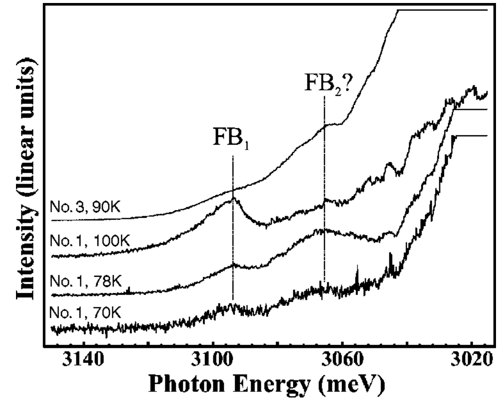

FIG. 6. Free-to-bound spectra. Each spectrum is labeled with the sample number and the temperature. FB_1 denotes the free-to-bound peak known from the literature, and FB_2 is our tentative assignment (thus the question mark).

the authors accept the same free-exciton binding energy for 4*H* as in 3*C*-SiC (27 meV), and obtain the value $E_A = 203$ meV for the Al acceptor. If the value 3287 is used for the electronic band gap, as in this paper, we obtain $E_A \approx 198$ meV, in close agreement with the result from the fit of the DAP spectrum.

Furthermore, we note the existence of the peak around 3065 meV, which has a similar line shape as the usual free-to-bound peak at 3093 meV. However, its assignment to free-to-bound transitions involving the deeper acceptor Al_k cannot be unambiguous because its position is very close to this for the B_0 peak shown in Fig. 2 (curve *a*), which might not be quenched completely at these temperatures. If this peak is indeed due to free-to-bound (to Al_k) transitions, then from the energy difference between the two peaks one obtains $E_{Ak} \approx 227$ meV, in good agreement with the result from the fit with the *hk* set. However, both the fit and this free-to-bound peak are to be considered as tentative, as already mentioned above.

In conclusion, it is worth mentioning two more arguments in favor of deeper Al_k level. First, there still exists some line structure on the low-energy side of the C_0 peak, where the (N_k-Al_k) recombination is anticipated in case of deeper Al_k level. And second, the usual photoluminescence of Al-doped samples clearly shows two peaks related to recombination of Al-bound excitons at the two inequivalent lattice sites. The exciton binding energies deduced from their peak positions are 17.3 and 18.8 meV. If the Haynes rule[27] holds for this acceptor in 4*H*-SiC, one would expect difference of at least 15 meV between E_{Ah} and E_{Ak}, which is not negligible.

V. CONCLUSION

We have shown that a fit of the DAP-PL spectrum is possible if the spectrum is modeled taking into account the features arising from the anisotropy and presence of inequivalent lattice sites in 4*H*-SiC. It is also shown that the recombination of pairs involving N donor and Al acceptor at hexagonal sites is dominating the spectrum. From the fit, the acceptor binding energy $E_{Ah} \approx 199$ meV can be obtained rather accurately (assuming the donor binding energy E_{Dh}

≈61.4 meV is known)[15] and compared to the value reported previously using free-to-bound transitions. However, the accuracy of this value depends on the accurate knowledge of the band gap taken in this paper as 3287 meV.[23]

ACKNOWLEDGMENTS

Okmetic AB is thanked for supplying some of the samples. Support from the SSF program SiCEP and the Swedish Research Council is gratefully acknowledged.

---

*Also at Okmetic AB, Hans Meijers väg 2, 583 30 Linköping, Sweden.

[1] L. Patrick, Phys. Rev. **188**, 1254 (1969).

[2] A.T. Vink, R.L.A. van der Heyden, and J.A.W. van der Does de Bye, J. Lumin. **8**, 105 (1973).

[3] J.J. Hopfield, D.G. Thomas, and M. Gershenzon, Phys. Rev. Lett. **10**, 162 (1963); D.G. Thomas, M. Gershenzon, and F.A. Trumbore, Phys. Rev. **133**, A269 (1964); F.A. Trumbore and D.G. Thomas, *ibid.* **137**, A1030 (1965).

[4] L. Patrick, Phys. Rev. Lett. **21**, 1685 (1968); Phys. Rev. **180**, 794 (1969).

[5] W.J. Choyke and L. Patrick, Phys. Rev. B **2**, 4959 (1970).

[6] Nguen Ngok Long, D.S. Nedzvetskii, N.K. Prokofeva, and M.B. Reifman, Opt. Spectrosc. **29**, 388 (1970).

[7] C.H. Henry, R.A. Faulkner, and K. Nassau, Phys. Rev. **183**, 798 (1969).

[8] D.C. Reynolds and T.C. Collins, Phys. Rev. **188**, 1267 (1969).

[9] S.H. Hagen, A.W.C. van Kemenade, and J.A.W. van der Does de Bye, J. Lumin. **8**, 18 (1973).

[10] M. Ikeda, H. Matsunami, and T. Tanaka, Phys. Rev. B **22**, 2842 (1980).

[11] P.J. Dean and L. Patrick, Phys. Rev. B **2**, 1888 (1970).

[12] M. Lax, J. Phys. Chem. Solids **8**, 66 (1959); Phys. Rev. **119**, 1502 (1960).

[13] L. L. Clemen, R. P. Devaty, W. J. Choyke, J. A. Powell, D. J. Larkin, J. A. Edmond, and A. A. Burk, in *The Proceedings of the 5th Conference on Silicon Carbide and Related Materials, 1–3 November 1993*, edited by M.G. Spencer, R.P. Devaty, J.A. Edmond, M. Asif Khan, R. Kaplan, and M. Rahman, IOP Conf. Proc. No. 137 (Institute of Physics, London, 1994), p. 297.

[14] I.S. Gorban, A.P. Krokhmal, V.I. Levin, A.S. Skirda, Yu.M. Tairov, and V.F. Tsvetkov, Fiz. Tekn. Poloprovdn. **21**, 194 (1987) [Sov. Phys. Semicond. **21**, 119 (1987)].

[15] I. G. Ivanov, B. Magnusson, and E. Janzén, Phys. Rev. B **67**, 165212 (2003).

[16] J. J. Hopfield, in *Proceedings of the International Conference on the Physics of Semiconductors, Dunod Cie., Paris, 1964* (Academic, NY, 1965)

[17] J.A.W. van der Does de Bye, A.T. Vink, A.J. Bosman, and R.C. Peters, J. Lumin. **3**, 185 (1970).

[18] D.G. Thomas, J.J. Hopfield, and W.M. Augustyniak, Phys. Rev. **140**, A202 (1965).

[19] Since the main contribution to the capture from remote pairs is due to capture of carriers to the excited states of the donor or acceptor, and the excited states do not exhibit such pronounced site dependence of their energies, we do not expect large differences in the capture cross section of remote pairs with any combination for the sites of the donor and the acceptor.

[20] G.F. Neumark, S.P. Herko, T.F. McGee III, and B.J. Fitzpatrick, Phys. Rev. Lett. **53**, 604 (1984).

[21] W.J. Choyke and L. Patrick, Phys. Rev. B **2**, 2255 (1970).

[22] A. Taylor, R. M. Jones, in *Silicon Carbide—A High Temperature Semiconductor,* edited by J. R. O'Connor and J. Smiltens (Pergamon, Oxford, 1960), p. 147.

[23] We consider the value 3287 meV as more probable than our previous estimate of 3286±1 meV, made in I. G. Ivanov, J. Zhang, L. Storasta, and E. Janzén, in *Proceedings of the International Conference on Silicon Carbide and Related Materials 2001* (Trans Tech, Switzerland, 2002), p. 613. The reason is that the excitonic band gap seems to be closer to 3266 than to 3265 meV, as taken in this reference.

[24] H. Kuwabara and S. Yamada, Phys. Status Solidi A **30**, 739 (1975).

[25] Nguen Ngok Long, D.S. Nedzvetskii, N.K. Prokofeva, and M.B. Reifman, Opt. Spectrosc. **30**, 165 (1971).

[26] S.G. Sridhara, L.L. Clemen, R.P. Devaty, W.J. Choyke, D.J. Larkin, H.S. Kong, T. Troffer, and G. Pensl, J. Appl. Phys. **83**, 7909 (1998).

[27] J.R. Haynes, Phys. Rev. Lett. **4**, 361 (1960).